# Deeply inelastic pions in the exclusive reaction $p(e, e'\pi^+)n$ above the resonance region

Murat M. Kaskulov,* Kai Gallmeister, and Ulrich Mosel

*Institut für Theoretische Physik, Universität Giessen, D-35392 Giessen, Germany*

(Dated: January 7, 2009)

A model for the $p(e, e'\pi^+)n$ reaction which combines an improved treatment of gauge invariant meson–exchange currents and hard deep–inelastic scattering (DIS) of virtual photons off nucleons is proposed. It is shown that DIS dominates and explains the transverse response at moderate and high photon virtualities $Q^2$ whereas the longitudinal response is dominated by hadronic degrees of freedom and the pion electromagnetic form factor. This leads to a combined description of the longitudinal and transverse components of the cross section in a wide range of photon virtuality $Q^2$ and momentum transfer to the target $t$ and solves the longstanding problem of the observed large transverse cross sections. The latter are shown to be sensitive to the intrinsic transverse momentum distribution of partons.

At Jefferson Laboratory (JLAB) the exclusive reaction $p(e, e'\pi^+)n$ has been investigated for a range of photon virtualities up to $Q^2 \simeq 5$ GeV$^2$ at an invariant mass of the $\pi^+ n$ system around the onset of deep–inelastic regime, $W \simeq 2$ GeV [1, 2, 3]. A separation of the cross section into the transverse $\sigma_\mathrm{T}$ and longitudinal $\sigma_\mathrm{L}$ components has been performed. The longitudinal cross section $\sigma_\mathrm{L}$ is well understood in terms of the pion quasi–elastic knockout mechanism [4] because of the pion pole at low $-t$ . This makes it possible to study the charge form factor of the pion at momentum transfer much bigger than in the scattering of pions from atomic electrons [5]. On the other hand, the $\sigma_\mathrm{T}$ is predicted to be suppressed by $\sim 1/Q^2$ with respect to $\sigma_\mathrm{L}$ for sufficiently high $Q^2 \gg \Lambda_\mathrm{QCD}^2$ [6].

However, the data from the $\pi$–$CT$ experiment [3] show that $\sigma_\mathrm{T}$ is large at JLAB energies. At $Q^2 = 3.91$ GeV$^2$ $\sigma_\mathrm{T}$ is by about a factor of two larger than $\sigma_\mathrm{L}$ and at $Q^2 = 2.15$ GeV$^2$ it has same size as $\sigma_\mathrm{L}$ in agreement with previous JLAB measurements [1]. Theoretically, the model of Ref. [7], which is generally considered to be a guideline for the experimental analysis and extraction of the pion form factor, underestimates $\sigma_\mathrm{T}$ at $Q^2 = 2.15$ GeV$^2$ and at $Q^2 = 3.91$ GeV$^2$ by about one order of magnitude [3]. Previous measurements at values of $Q^2 = 1.6$ (2.45) GeV$^2$ [1] show a similar problem in the understanding of $\sigma_\mathrm{T}$. Even at smaller JLAB [2] and much higher Cornell [8] values of $Q^2$ there is a disagreement between model calculations based on the hadron–exchange scenario and experimental data; see Ref. [9] for a possible interpretation and references therein.

In this work we first generalize the treatment of Ref. [7] for the longitudinal contribution. We then propose a resolution of the $\sigma_\mathrm{T}$ problem. The idea followed here is to complement the soft hadron–like interaction types shown in Figure 1 which dominate in photoproduction and low $Q^2$ electroproduction by direct hard interaction of vir-

tual photons with partons followed by the hadronization process into $\pi^+ n$ channel, to form the $\pi^+$– electroproduction framework. As we shall show, then the large $\sigma_\mathrm{T}$ in the reaction $p(e, e'\pi^+)n$ can be readily explained and both $\sigma_\mathrm{L}$ and $\sigma_\mathrm{T}$ can be described from low up to high values of $Q^2$.

The exclusive reaction

$$e(P_e) + N(p) \rightarrow e'(P'_e) + \pi(k') + N(p') \qquad (1)$$

with unpolarized electrons is described by four structure functions $\sigma_\mathrm{T}$, $\sigma_\mathrm{L}$, $\sigma_\mathrm{LT}$ and $\sigma_\mathrm{TT}$ [10]. After the integration over the azimuthal angle between the leptonic and hadronic scattering planes only $\sigma_\mathrm{T}$ and $\sigma_\mathrm{L}$ remain and the differential cross section takes the form

$$d\sigma_e/dQ^2 d\nu dt = \frac{\pi \, \Phi}{E_e(E_e - \nu)} \left[ d\sigma_\mathrm{T}/dt + \varepsilon d\sigma_\mathrm{L}/dt \right], (2)$$

where $\varepsilon$ is the virtual photon polarization. The definition of the virtual photon flux $\Phi$ follows the convention of Ref. [10]. The subscripts T and L denote the projections of the $(\gamma^*, \pi)$ amplitude onto the basis vectors $\epsilon_\mu^\lambda$ of the circular polarization of the virtual photon quantized along its three momentum $\vec{q}$: T– transverse ($\lambda = \pm 1$) and L– longitudinal ($\lambda = 0$) polarizations.

At first we consider the soft hadron–exchange part of the $\pi^+$–electroproduction amplitude. In Figure 1 the Feynman diagrams describing the high energy $\pi^+$ electroproduction in the hadron–exchange approach are shown. It has been well known for a long time that the $\pi$–pole amplitude, first diagram in Figure 1, gives the dominant contribution to the longitudinal response $\sigma_\mathrm{L}$. The $\pi$–pole amplitude by itself is not gauge invariant and charge conservation requires an addition of the electric part of the $s$–channel nucleon Born term (third diagram in Figure 1) [7, 11]. When considering realistic vertex functions, which include form factors, current conservation is violated and one has to restore the gauge invariance of the model [12]. A simple solution to this problem is to choose all of the electromagnetic form factors to be the same [7]. However, it is experimentally known that

---

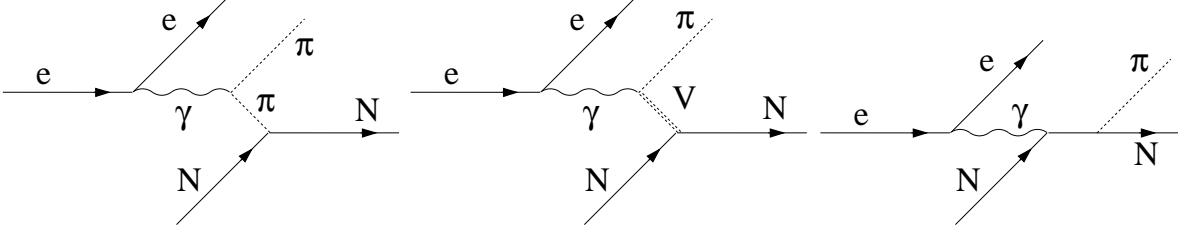*Electronic address: Murat.Kaskulov@theo.physik.uni-giessen.de

FIG. 1: The diagrams describing the hadronic part of the $\pi^{+-}$ electroproduction amplitude at high energies. See text for the details.

these form factors are not the same and have different scaling behavior $F_{\gamma\pi\pi} \sim 1/Q^2$ for the pion form factor and $F_1^p \sim 1/Q^4$ for the proton Dirac form factor.

In the following we use the Regge pole model of Ref. [7] which is based on the same set of Born diagrams but concerning the electromagnetic form factors we employ a prescription proposed in Refs. [13, 14] where an arbitrary form factor $F(Q^2)$ can be accommodated by the following replacement of the currents

$$\Gamma^\mu \to \Gamma'^\mu(Q^2) = \Gamma^\mu + [F(Q^2) - 1]\,\mathcal{P}_\perp^{\mu\nu}\Gamma_\nu\,, \quad (3)$$

where $\mathcal{P}_\perp^{\mu\nu} = g^{\mu\nu} - q^\mu q^\nu/q^2$ stands for the projector into the 3-dimensional transverse subspace. This procedure guarantees that the resulting current $\Gamma'^\mu$ obeys the same Ward–Takahashi identities as $\Gamma^\mu$. Thus, and as long as gauge invariance is implemented for real photons, one can use the experimentally determined form factors in the $\pi$–pole $J_\pi^\mu$ and $s$–channel nucleon Born $J_s^\mu$ currents and still retain gauge invariance for arbitrary $Q^2$.

Making use of Eq. (3) the $\gamma\pi\pi$ and $\gamma NN$ vertex functions are given by

$$\Gamma_{\gamma\pi\pi}^\mu = e\,(k + k')^\mu + e\,[F_{\gamma\pi\pi}(Q^2) - 1]\,\mathcal{P}_\perp^{\mu\nu}(k + k')_\nu, \quad (4)$$

$$\Gamma_{\gamma NN}^\mu = e\,\gamma^\mu + e\,[F_1^N(Q^2) - 1]\,\mathcal{P}_\perp^{\mu\nu}\gamma_\nu, \quad (5)$$

where the four momentum vectors of pions are $k$ (incoming) and $k'$ (outgoing). In Eq. (4) we have - as usual - assumed that the half–off–shell form factor $F_{\gamma\pi\pi}(Q^2, t)$ depends only on $Q^2$. Using Eqs. (4) and (5) the gauge invariant hadronic current $J^\mu$ describing the reaction $p(\gamma^*, \pi^+)n$ is constructed as a sum $J^\mu = J_\pi^\mu + J_s^\mu$.

At high energies the exchange of high–spin and high–mass particles has to be taken into account. To account for these states we replace in $J_\pi^\mu$ the $\pi$–Feynman propagator by the Regge propagator [7]. Furthermore, since the $s$–channel Born term can generate the pion pole itself [11], we factor out the pion propagator in the sum $J_\pi^\mu + J_s^\mu$ following Ref. [7] and reggeize it according to the above prescription. The hadronic current which satisfies the current conservation, i.e. $q_\mu J^\mu = 0$, takes the form

$$-iJ^\mu = \sqrt{2}g_{\pi NN}\,\bar{u}_{s'}(p')\gamma_5 \left[ F_{\gamma\pi\pi}(Q^2)\frac{(k + k')^\mu}{t - m_\pi^2 + i0^+} \right.$$

$$\left. + F_1^p(Q^2)\frac{k'_\sigma\gamma^\sigma\gamma^\mu}{W^2 - M_p^2 + i0^+} \right.$$

$$\left. + [F_{\gamma\pi\pi}(Q^2) - F_1^p(Q^2)]\frac{(k - k')^\mu}{Q^2} \right] u_s(p)$$

$$\times [t - m_\pi^2 + i0^+]\left(\frac{W}{W_0}\right)^{2\alpha_\pi(t)}\frac{\pi\alpha'_\pi}{\sin(\pi\alpha_\pi(t))}\frac{e^{-i\pi\alpha_\pi(t)}}{\Gamma(1 + \alpha_\pi(t))}, \quad (6)$$

where

$$\alpha_\pi(t) = \alpha_\pi^0 + \alpha'_\pi t = 0.7(t - m_\pi^2) \quad (7)$$

is the degenerate $\pi$–$b_1$–trajectory, $W_0 = 1$ GeV and the Gamma function $\Gamma$ suppresses the singularities in the physical region ($t < 0$). In Eq. (6) $g_{\pi NN} = 13.4$ is the pseudoscalar $\pi N$ coupling constant, $t = k^2$, $k = k' - q = p - p'$ and other notations are obvious. It should be noted that in the current (6) the two different form factors of the nucleon and the pion appear; this is in contrast to the work of [7] where these two form factors $F_{\gamma\pi\pi}$ and $F_1^p$ were assumed to be identical in order to reach gauge invariance. For the pion charge form factor we use a monopole parameterization

$$F_{\gamma\pi\pi}(Q^2) = (1 + Q^2/\Lambda_{\gamma\pi\pi}^2)^{-1}, \quad (8)$$

with the cut–off $\Lambda_{\gamma\pi\pi}$ as a fit parameter. The Dirac form factor $F_1^p(Q^2)$ is described by a standard dipole form.

The second diagram in Figure 1 describes the exchange of the $\rho$–meson Regge trajectory. The current $J_\rho^\mu$ reads

$$-iJ_\rho^\mu = -i\sqrt{2}\,G_{\rho NN}G_{\gamma\rho\pi}F_{\gamma\rho\pi}(Q^2)\varepsilon^{\mu\nu\alpha\beta}q_\nu k_\alpha$$

$$\times \bar{u}_{s'}(p')\left[(1 + \kappa_\rho)\gamma_\beta - \frac{\kappa_\rho}{2M_p}(p + p')_\beta\right]u_s(p)$$

$$\times \left(\frac{W}{W_0}\right)^{2\alpha_\rho(t)-2}\frac{\pi\alpha'_\rho}{\sin(\pi\alpha_\rho(t))}\frac{e^{-i\pi\alpha_\rho(t)}}{\Gamma(\alpha_\rho(t))}. \quad (9)$$

The parameters needed for the proper description of the current $J_\rho^\mu$ are

$$\alpha_\rho(t) = 0.55 + 0.8t \quad (10)$$

as the degenerate $\rho$–$a_2$–trajectory, $G_{\rho NN} = 3.1$ is the vector and $\kappa_\rho = 6.1$ is the tensor $\rho N$ coupling constants. The $\gamma\rho\pi$ coupling constant $G_{\gamma\rho\pi} = 0.728$ GeV$^{-1}$ has been deduced from the decay width [15]

$$\Gamma_{\rho^+ \to \pi^+\gamma} \simeq 67.5 \text{ keV}. \quad (11)$$

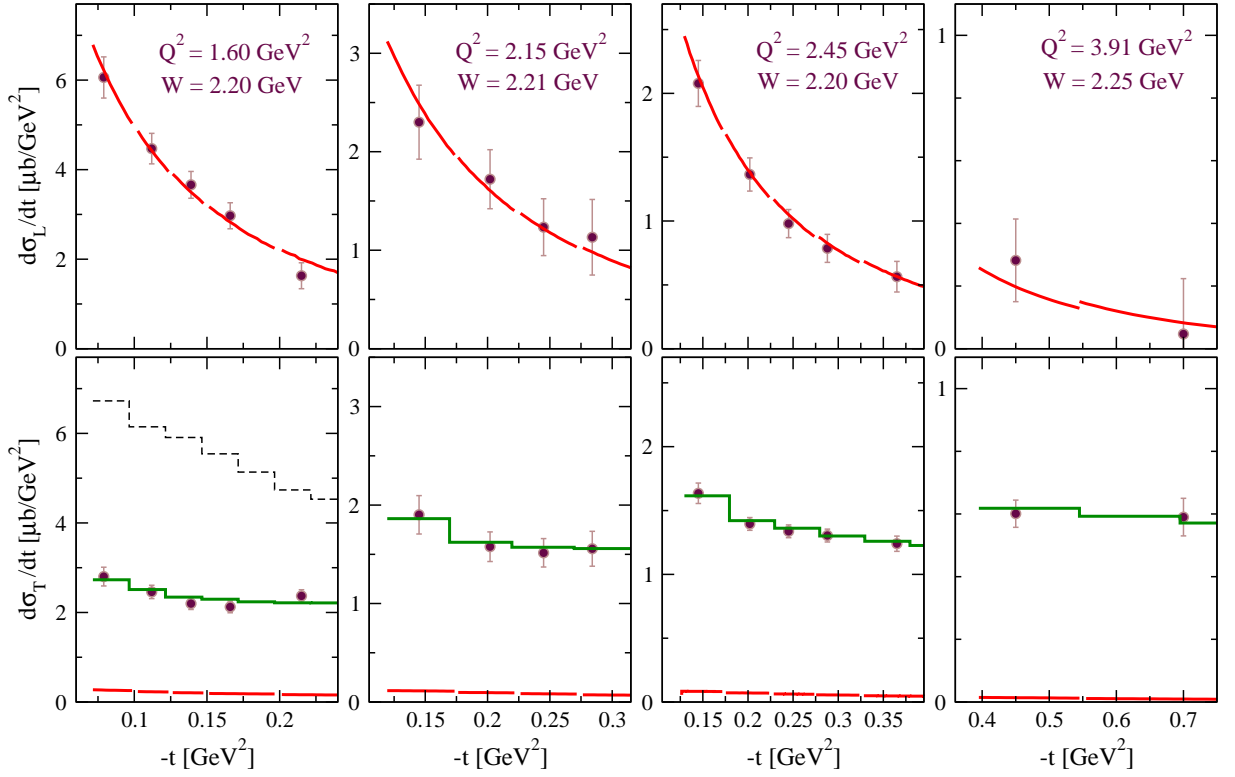For the $\gamma\rho\pi$ vertex form factor $F_{\gamma\rho\pi}$ we use the prediction of Ref. [16].

FIG. 2: The longitudinal $d\sigma_{\rm L}/dt$ (top panels) and transverse $d\sigma_{\rm T}/dt$ (bottom panels) differential cross sections of the reaction $p(\gamma^*, \pi^+)n$ at average values of $Q^2 = 1.60$ (2.45) GeV$^2$ [1] and $Q^2 = 2.15$ (3.91) GeV$^2$ [3]. The solid curves are the contribution of the hadron–exchange model and the histograms are the contribution of the DIS pions. The discontinuities in the curves result from the different values of $Q^2$ and $W$ for the various $-t$ bins. The dashed histogram in the lower left panel shows the contribution of the DIS pions for the average transverse momentum of partons $\sqrt{\langle k_{\rm t}^2 \rangle} = 0.4$ GeV.

In Figure 2 the results for the $p(\gamma^*, \pi^+)n$ differential cross sections $d\sigma_{\rm L}/dt$ (top panels) and $d\sigma_{\rm T}/dt$ (bottom panels) are compared with the data from JLAB $F\pi$–2 [1] and $\pi$–$CT$ [3] experiments. The longitudinal cross section $d\sigma_{\rm L}/dt$ is very well described by the hadron–exchange model (solid curves) with the cut–off in the pion form factor being fixed to the constant value $\Lambda^2_{\gamma\pi\pi} = 0.52$ GeV$^2$. The discontinuities in the curves result from the different values of $Q^2$ and $W$ for the various $-t$ bins. The steep fall of $d\sigma_{\rm L}/dt$ away from forward angles comes entirely from the rapidly decreasing $\pi$–pole amplitude. The interference of this amplitude with the $s$–channel nucleon Born term is minimized due to the presence of different form factors for both amplitudes. The contribution of the natural parity $\rho$–exchange is negligible in $\sigma_{\rm L}$ and $\sigma_{\rm T}$.

This comparison with data shows that $F_{\gamma\pi\pi}$ can indeed be reliably extracted from the longitudinal data.

Again, the model strongly underestimates $d\sigma_{\rm T}/dt$, for example, at $Q^2 = 1.6$ GeV$^2$ by a factor of 10 and at $Q^2 = 3.91$ GeV$^2$ by a factor of 30. This is also seen in the model of Ref. [7], although somewhat less pronounced [1, 3].

The solution to this problem is still missing. One might describe this transverse strength in the language of perturbative QCD by considering higher twist corrections to

a GPD based handbag diagram. However, such a calculation does not exist and it is not clear if a higher–twist expansion converges in the kinematical regime considered here. Our solution of this problem, therefore, is to model such effects. We start from the observation that the second term of Eq. (6) contributes very little to both the longitudinal and transverse cross sections. Here only the nucleon Born term is taken into account to conserve the charge of the system. However, at the invariant masses reached in the experiment ($W \approx 2.2$ GeV) nucleon resonances can contribute to the $1\pi$ channel. Similar to the replacement above of the pion propagator by a Regge propagator that takes higher meson excitations into account we now complement the $s$–channel nucleon Born term with direct hard interaction of virtual photons with partons (DIS) since DIS involves all possible transitions of the nucleon from its ground state to any excited state [17]. Note, that our suggestion concerning the partonic contribution follows the qualitative arguments in [18] where it has been shown that the typical exclusive photoproduction mechanisms involving a peripheral quark–antiquark pair in the proton wave function, the $t$–channel meson–exchange processes considered above, should be unimportant in the transverse response already around $Q^2 \gtrsim 1$ GeV$^2$ and play no role in the true deep inelastic region. This we have already seen in

Figure 2.

The total transverse DIS cross section reads

$$\sigma_{\mathrm{T}}^{\mathrm{DIS}} = \frac{4\pi^2\alpha}{1-x}\frac{F_1^p(x,Q^2)}{\nu M_p} = \frac{4\pi^2\alpha}{1-x}\frac{F_2^p(x,Q^2)}{Q^4}\frac{Q^2+4M_p^2x^2}{1+\mathcal{R}(x,Q^2)},$$ (12)

where $\alpha \simeq \frac{1}{137}$ and $x = \frac{Q^2}{2\nu M_p}$. In the following we assume that a partonic description of deep–inelastic structure functions $F_{1(2)}^p(x,Q^2)$ works well not only in the Bjorken limit where $\mathcal{R} \equiv \sigma_{\mathrm{L}}^{\mathrm{DIS}}/\sigma_{\mathrm{T}}^{\mathrm{DIS}}$ tends to zero but is valid down to values of $Q^2$ considered in Figure 2.

To determine the structure of events in DIS a model for the hadronization process is needed. Furthermore, since at JLAB (Bjorken $x \gtrsim 0.3$) the antiquark content of the structure functions becomes negligible, we model the DIS by the $\gamma^*q \to q$ knockout reaction followed by hadronization through string fragmentation. In the present description of hadronization in DIS we rely on the Lund model (LM) [19] as depicted in Figure 3 where the $\gamma^*q \to q$ process followed by the fragmentation of an excited colored string (wavy curve connecting the quark lines[1]) into two particles ($\pi N$) is shown. The LM predicts two jets for the $\pi^+n$ final state in the forward and backward directions. As a realization of the LM in DIS we use the PYTHIA/JETSET implementation [20]. The LM involves parameters which have been tuned in different fragmentation channels. Our approach here is to modify as few parameters as possible compared to the default set of values [20] which describes the $\pi^+$ SIDIS spectra measured at JLAB [21] remarkably well. Since in PYTHIA the average transverse momentum of partons $\sqrt{\langle k_t^2 \rangle}$ cannot be fixed from first principles and since it affects the slope and magnitude of $d\sigma_{\mathrm{T}}/dt$ at forward angles we choose this as a free parameter. Therefore, one has to regard the average $\sqrt{\langle k_t^2 \rangle}$ used here as an effective parameter which is tuned to obtain an agreement with data. However, for consistency we use the same value for $\sqrt{\langle k_t^2 \rangle}$ in all kinematic regimes together with the default JETSET parameters. As pointed out above we view the string fragmentation process as an effective model for higher–order twist effects, for example in GPD based handbag calculations. The success of our description may then be taken as an indication that the string fragmentation process described in JETSET works well down to the rather low invariant mass of about 2 GeV where the individual nucleon resonances tend to disappear.

The lower part of Figure 2 shows that $d\sigma_{\mathrm{T}}/dt$ receives the dominant contribution from DIS fragmentation pions (solid histograms). In Eq. (12) for $F_2^p$ we use the fit of Ref. [22] and for $\mathcal{R}$ the parameterization of Ref. [23] has been employed. In [20] the value of $\sqrt{\langle k_t^2 \rangle} = 1.2$ GeV has been used for all $Q^2$ bins; this value is close to the default PYTHIA value of $\sqrt{\langle k_t^2 \rangle} = 1$ GeV and well within the com-
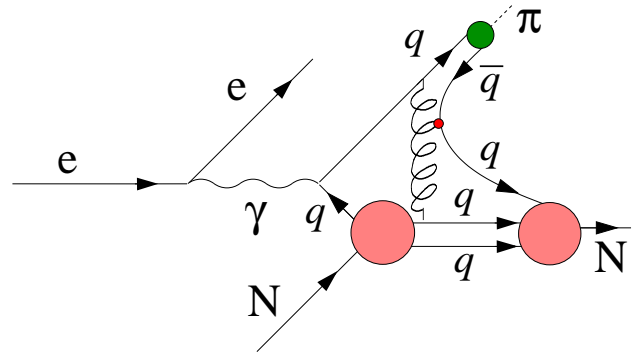


FIG. 3: A schematic representation of the partonic part of the $\pi-$ electroproduction mechanism. The wavy line represents a color string. See text for the details.

mon range of transverse momentum distributions [24]. As one can see in Figure 2 (bottom panels) the absolute value and the $-t$ dependence of $d\sigma_{\mathrm{T}}/dt$ are very well reproduced. A decrease of $\sqrt{\langle k_t^2 \rangle}$ increases the slope and magnitude of $d\sigma_{\mathrm{T}}/dt$ at forward angles. In Figure 2 this is shown for $\sqrt{\langle k_t^2 \rangle} = 0.4$ GeV (dashed histogram).

We have also compared the model results with data from the JLAB $F\pi-1$ experiment [2] at lower values of $Q^2$. Also here we find that an addition of the DIS pions describes the experimental data very well. However, contrary to the situation at higher values of $Q^2$ where the hadronic part gives only a marginal contribution to $\sigma_{\mathrm{T}}$, at low $Q^2$ the problem of double counting arises when using both the DIS and the Regge contributions to the transverse cross section. Following Ref. [25] this could be solved by turning off the leading order DIS contribution, as required by gauge invariance for $\gamma^*q \to q$, when approaching the photon point where the Regge description alone gives a good description of data [7]. In the calculation presented here the transverse part is solely generated by the DIS process (12) without any further modification.

In Figure 4 we confront the result of our calculations (solid curves) with the new JLAB data [26] for unseparated cross sections at average value of $W \simeq 2.2$ GeV. The data are very well described by the present model in a measured range from $Q^2 \simeq 1$ GeV$^2$ up to 5 GeV$^2$. Furthermore, assuming that the exclusive cross section behaves as $\sigma_{\mathrm{T}}^{\mathrm{DIS}}(Q^2) \propto F_1^p(x,Q^2)$ in Eq. (12) [2] and that the ratio $\mathcal{R}$ is small or nearly the same both for protons and neutrons we predict then a smaller transverse cross section in the reaction $n(e,e'\pi^-)p$ off neutrons, i.e.

$$\sigma_{\mathrm{T}}^n/\sigma_{\mathrm{T}}^p \simeq F_1^n/F_1^p \approx F_2^n/F_2^p < 1,$$ (13)

while because of the $\pi$–pole dominance

$$\sigma_{\mathrm{L}}^n/\sigma_{\mathrm{L}}^p \simeq 1.$$ (14)

---

[1] Not to be confused with the perturbative one gluon exchange.

[2] This behavior has been already noticed in [8] from a fit to data and is supported by the present model.
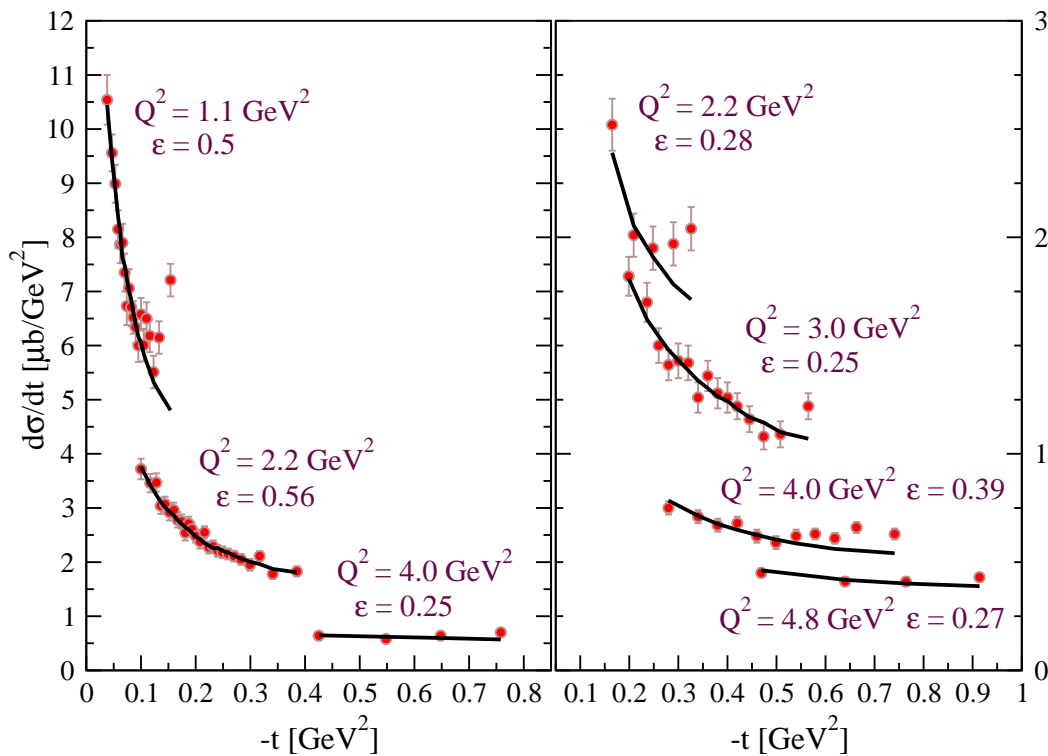
FIG. 4: Differential cross section $d\sigma/dt = d\sigma_{\mathrm{T}}/dt + \varepsilon d\sigma_{\mathrm{L}}/dt$ of the reaction $p(\gamma^*, \pi^+)n$. The solid curves are the model predictions. The experimental data are from Ref. [26].

A preliminary analysis in Ref. [1] has shown that the latter ratio is indeed consistent with unity and $\sigma_{\mathrm{L}}/\sigma_{\mathrm{T}}$ must be larger for $\pi^-$ than for $\pi^+$. This, together with the fact that $\sigma_{\mathrm{L}}$ is described very well also at the highest $Q^2$ by the Regge picture alone indicates that the DIS contribution to the exclusive longitudinal channel must be small.

In summary, in this work we have extended the earlier model of Ref. [7] such that the electromagnetic form factor of the pion and the nucleon no longer have to be set equal in order to achieve gauge invariance. In addition, we have proposed a resolution of the $\sigma_{\mathrm{T}}$ problem in the reaction $p(e, e'\pi^+)n$ above the resonance region. A model which combines the gauge invariant hadron–exchange currents and DIS of virtual photons off partons has been proposed. The model with hadronic states as the active degrees of freedom describes the longitudinal cross section $\sigma_{\mathrm{L}}$ very well and exhibits the dominance of the $\pi$–pole mechanism while $\sigma_{\mathrm{T}}$ is grossly underestimated. We have shown that the description of $\sigma_{\mathrm{T}}$ at values of $Q^2 > 1$ GeV$^2$ requires a proper inclusion of the hard scattering processes and that $\gamma^* q \to q$ followed by the $\pi^+ n$ fragmentation of the nucleon may naturally explain the large transverse cross section observed at JLAB. The model can be used for the extraction of the pion form factor from high energy pion electroproduction data with longitudinally polarized photons. The sensitivity of the transverse cross section to the transverse $\sqrt{\langle k_{\mathrm{t}}^2 \rangle}$ of partons can be used to reduce the theoretical uncertainties in the interpretation of the color transparency signal observed at JLAB in the reaction $(e, e'\pi^+)$ off nuclei [27, 28]. Finally, we mention another $\sigma_{\mathrm{L}}/\sigma_{\mathrm{T}}$ puzzle in the reaction $p(e, e'K^+)\Lambda(\Sigma)$ [29] which may apparently get a similar solution [30].

[1] T. Horn *et al.*, Phys. Rev. Lett. **97**, 192001 (2006).
[2] V. Tadevosyan *et al.*, Phys. Rev. C **75**, 055205 (2007).
[3] T. Horn *et al.*, arXiv:0707.1794 [nucl-ex].
[4] V. G. Neudatchin *et al.*, Nucl. Phys. A **739**, 124 (2004).
[5] J. D. Sullivan, Phys. Lett. B **33**, 179 (1970).
[6] J. C. Collins, L. Frankfurt and M. Strikman, Phys. Rev. D **56**, 2982 (1997).
[7] M. Vanderhaeghen, M. Guidal and J. M. Laget, Phys. Rev. C **57**, 1454 (1998); M. Guidal, J. M. Laget and M. Vanderhaeghen, Nucl. Phys. A **627**, 645 (1997).

[8] C. J. Bebek *et al.*, Phys. Rev. D **17**, 1693 (1978).

[9] A. Faessler *et al.*, Phys. Rev. C **76**, 025213 (2007).

[10] L. N. Hand, Phys. Rev. **129**, 1834 (1963).

[11] L. M. Jones, Rev. Mod. Phys. **52**, 545 (1980).

[12] H. Naus and J. H. Koch, Phys. Rev. C **39**, 1907 (1989).

[13] J. H. Koch, V. Pascalutsa and S. Scherer, Phys. Rev. C **65**, 045202 (2002).

[14] F. Gross and D. O. Riska, Phys. Rev. C **36**, 1928 (1987).

[15] W. M. Yao *et al.*, Journal of Physics, **G 33**, 1 (2006).

[16] P. Maris and P. Tandy, Phys. Rev. C **65**, 045211 (2002).

[17] F. E. Close and N. Isgur, Phys. Lett. B **509**, 81 (2001).

[18] O. Nachtmann, Nucl. Phys. B **115**, 61 (1976).

[19] B. Andersson *et al.*, Phys. Rept. **97**, 31 (1983).

[20] T. Sjostrand *et al.*, JHEP **0605**, 026 (2006).

[21] H. Avakian *et al.*, Phys. Rev. D **69**, 112004 (2004).

[22] H. Abramowicz and A. Levy, arXiv:hep-ph/9712415.

[23] V. Tvaskis *et al.*, Phys. Rev. Lett. **98**, 142301 (2007).

[24] F. E. Close, F. Halzen and D. M. Scott, Phys. Lett. B **68**, 447 (1977).

[25] C. Friberg and T.Sjostrand, Phys.Lett. B**492**, 123 (2000).

[26] X. Qian *et al.*, to be submitted to Phys. Rev. C.

[27] B. Clasie *et al.*, Phys. Rev. Lett. **99**, 242502 (2007).

[28] M. M. Kaskulov, K. Gallmeister and U. Mosel, arXiv:0808.2564 [nucl-th].

[29] R. Mohring et al., Phys. Rev. C **67**, 055205 (2003).

[30] M. Kaskulov and U. Mosel, to be published.